Cell type-specific contributions to a persistent aggressive internal state in female *Drosophila*

Hui Chiu[1,✉*], Alice A. Robie[2], Kristin M. Branson[2], Tanvi Vippa[2], Samantha Epstein[2], Gerald M. Rubin[2,✉], David J. Anderson[1,3,✉], and Catherine E. Schretter[2,✉*]

[1]Division of Biology and Biological Engineering, Tianqiao and Chrissy Chen Institute for Neuroscience, California Institute of Technology, Pasadena, CA 91125, USA
[2]Janelia Research Campus, Howard Hughes Medical Institute, Ashburn, VA 20147, USA
[3]Howard Hughes Medical Institute, California Institute of Technology, Pasadena, CA 91125, USA
[*]These authors contributed equally to this work

Abstract

Persistent internal states are important for maintaining survival-promoting behaviors, such as aggression. In female *Drosophila melanogaster*, we have previously shown that individually activating either aIPg or pC1d cell types can induce aggression. Here we investigate further the individual roles of these cholinergic, sexually dimorphic cell types, and the reciprocal connections between them, in generating a persistent aggressive internal state. We find that a brief 30-second optogenetic stimulation of aIPg neurons was sufficient to promote an aggressive internal state lasting at least 10 minutes, whereas similar stimulation of pC1d neurons did not. While we previously showed that stimulation of pC1e alone does not evoke aggression, persistent behavior could be promoted through simultaneous stimulation of pC1d and pC1e, suggesting an unexpected synergy of these cell types in establishing a persistent aggressive state. Neither aIPg nor pC1d show persistent neuronal activity themselves, implying that the persistent internal state is maintained by other mechanisms. Moreover, inactivation of pC1d did not significantly reduce aIPg-evoked persistent aggression arguing that the aggressive state did not depend on pC1d-aIPg recurrent connectivity. Our results suggest the need for alternative models to explain persistent female aggression.

internal state | aggression | *Drosophila melanogaster*

Correspondence:
hui.chiu@yale.edu,
rubing@janelia.hhmi.org,
wuwei@caltech.edu,
schretterc@janelia.hhmi.org

Introduction

Persistence is an evolutionarily conserved feature of internal states, which governs the duration of an animal's behavior beyond an inciting stimulus (3, 4). For example, a glance at a moving muleta is sufficient to keep a Spanish fighting bull aggressive for tens of minutes. Recent studies in mammals and invertebrates have begun to uncover potential mechanisms for maintaining persistent behavioral states on various timescales. These mechanisms can be "electronic," such as persistent firing in certain cell types or circuits, "biochemical," such as slow decay of second messengers or their effectors influencing neural excitability, or "systemic," such as persistent elevation of circulating hormones or neuromodulators, and may span timescales of hundreds of milliseconds to tens of seconds to days (1, 5–11). In studies of working memory in mice, persistent neural activity generated by a recurrent

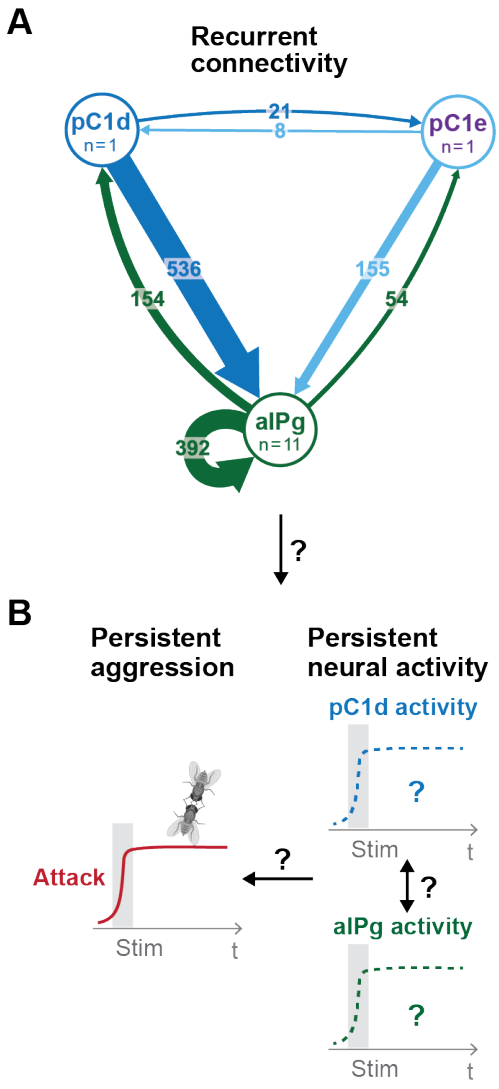

Fig. 1. Proposed model for persistent aggressive behavior in females. Recurrent connectivity between pC1d, pC1e, and aIPg (A) has been proposed to generate a persistent aggressive internal state by prolonging the neural activity of pC1d or aIPg neurons (B) (1, 2). For the connectivity diagram (A), synapse number is noted on each arrow and no thresholds were applied between types.

excitatory network has been proposed to sustain an animal's delayed response to a transient stimulation (12–15). However, circuit mechanisms that generate a persistent aggressive state remain unresolved (16). *Drosophila melanogaster* has been a useful model for discovering cell types that control aggression (reviewed in (17, 18)). Whether recurrent connectivity generates persistent neural activity that sustains prolonged aggression (Figure 1) is now a testable hypothesis due to recent advances in fly connectomics (19, 20).

In *Drosophila* males, most aggression-promoting neurons described thus far are male-specific, limiting the applicability of the available female fly connectome for addressing this question (21). However recent progress in identifying cell types that control female aggression has opened up this possibility (1, 2, 22, 23). Through behavioral screens and connectomic mapping, two groups independently showed that combined optogenetic activation of *doublesex* (*dsx*)-expressing pC1d and pC1e neurons promotes aggression in females (1, 2). Upon co-stimulation of pC1d and pC1e for either 2 or 5 minutes, Deutsch et al. (2020) observed persistent aggression and prolonged neuronal activity in subsets of *fruitless* (*fru*)- and *dsx*-expressing neurons (Supplementary Figure 1). As these experiments were performed using a GAL4 line labeling both pC1d and pC1e neurons, the individual roles of pC1d or pC1e in the maintenance of persistent aggression could not be determined.

In an independent study, Schretter et al. (2020) stimulated GAL4 lines that separately labeled pC1d and pC1e neurons, as well as those that co-labeled both pC1d and pC1e, to test their effects on female aggression. They observed that activation of pC1d neurons alone generated only time-locked aggression, while stimulation of pC1e had no effect on aggression at all (Supplementary Figure 1 and 2). Schretter et al. (2020) also identified an additional female aggression-promoting cell type, aIPg, not directly tested in Deutsch et al. (2020). They observed that a 30 second stimulation of aIPg neurons, like that of pC1d+e neurons, promoted aggression that outlasted the stimulation period. However, as individual flies were not separated during the stimulation period this study could not definitively conclude that stimulation of aIPg neurons generated a persistent aggressive internal state (2).

These two studies, therefore, raised a number of questions about the mechanisms generating persistent aggressive internal states in female flies. For example, can stimulation of pC1d alone generate a persistent internal aggressive state or is pC1e needed in combination with pC1d to see this long-lasting effect? Does the duration of the persistent state depend on the type of neuron stimulated (aIPg vs. pC1d+e), the duration of stimulation, or on other factors? It is difficult to answer these questions by combining the results of Deutsch et al. (2020) and Schretter et al. (2020), due to experimental differences between the two studies. For example, Deutsch et al. (2020) used males as targets of female aggressors while Schretter et al. (2020) used females as targets, and the two studies used different optogenetic stimulation conditions (partly summarized in Supplementary Figure 1). In this report, we evaluate the contribution of individual cell types, specifically aIPg, pC1d, and pC1e, to generating a persistent aggressive state, under directly comparable stimulation and behavioral assay conditions, and begin to test predictions of connectome-based models for circuit mechanisms underlying persistence.

Results

Stimulation of aIPg neurons but not pC1d neurons promotes a persistent aggressive state in females. We used a well-established behavioral test for evaluating persistent aggressive internal states (1, 19), in which same-genotype flies expressing the red-shifted channelrhodopsin, CsChrimson (CsChR), in the specified neuronal population were separated by a sliding metal door (Figure 2A). Therefore, their social interactions were withheld until the doors were removed at the desired time following neuronal stimulation. This design minimizes the influence of social feedback on internal state and thereby allows us to directly assess specific neuronal stimulation effects on the duration of a fly-autonomous internal aggressive state.

A 30-second 5 Hz 655 nm stimulation was applied to activate distinct neuronal populations: aIPg, pC1d, or pC1d+e (pC1d and pC1e together; the pC1d+e driver is designated as pC1-A in (1)). The driver lines marking these specific cell types were previously characterized in (2) and show similar levels of expression. Moreover, in all cases, the strength of the optogenetic stimulus used to test for persistence was similar to that needed to induce aggression during stimulation. Ten minutes following the stimulation, the doors were removed to allow social interactions (Figure 2A). Preliminary experiments using 1-, 5-, 10-, and 30-minute delays showed persistence at 1, 5 and 10 minutes, but not at 30 minutes; therefore, we performed more detailed experiments at the 10-minute time point. Aggressive behaviors such as head butting and shoving were analyzed using the Caltech FlyTracker and a JAABA classifier (Table 1). We observed elevated female aggression that was detectable after 10 minutes when aIPg or pC1d+e, but not pC1d neurons, were stimulated, suggesting that the aIPg neurons alone are sufficient to promote a persistent aggressive internal state. In contrast, pC1d depends on co-stimulation with pC1e to generate a persistent effect (Figure 2B-C). Because stimulation of pC1e neurons alone does not produce female aggression (2), its contribution to the regulation of the persistent aggression was unexpected. Collectively, these results demonstrate the sufficiency of either aIPg or pC1d+e neurons to promote a persistent aggressive state in females.

Using a different experimental paradigm, we next investigated whether social feedback from a less aggressive (group housed, as shown in (22)) wild-type target fly can contribute to the duration of persistent aggression. In this "mixed pair" assay, CsChrimson-expressing females were paired with wild-type female targets in chambers without a divider, allowing for social interactions at any time (Supplementary Figure 3). Under these conditions, attacks by the tester fly persisted following the stimulation of aIPg or pC1d+e, but not of pC1d. Activation of pC1e alone did not significantly

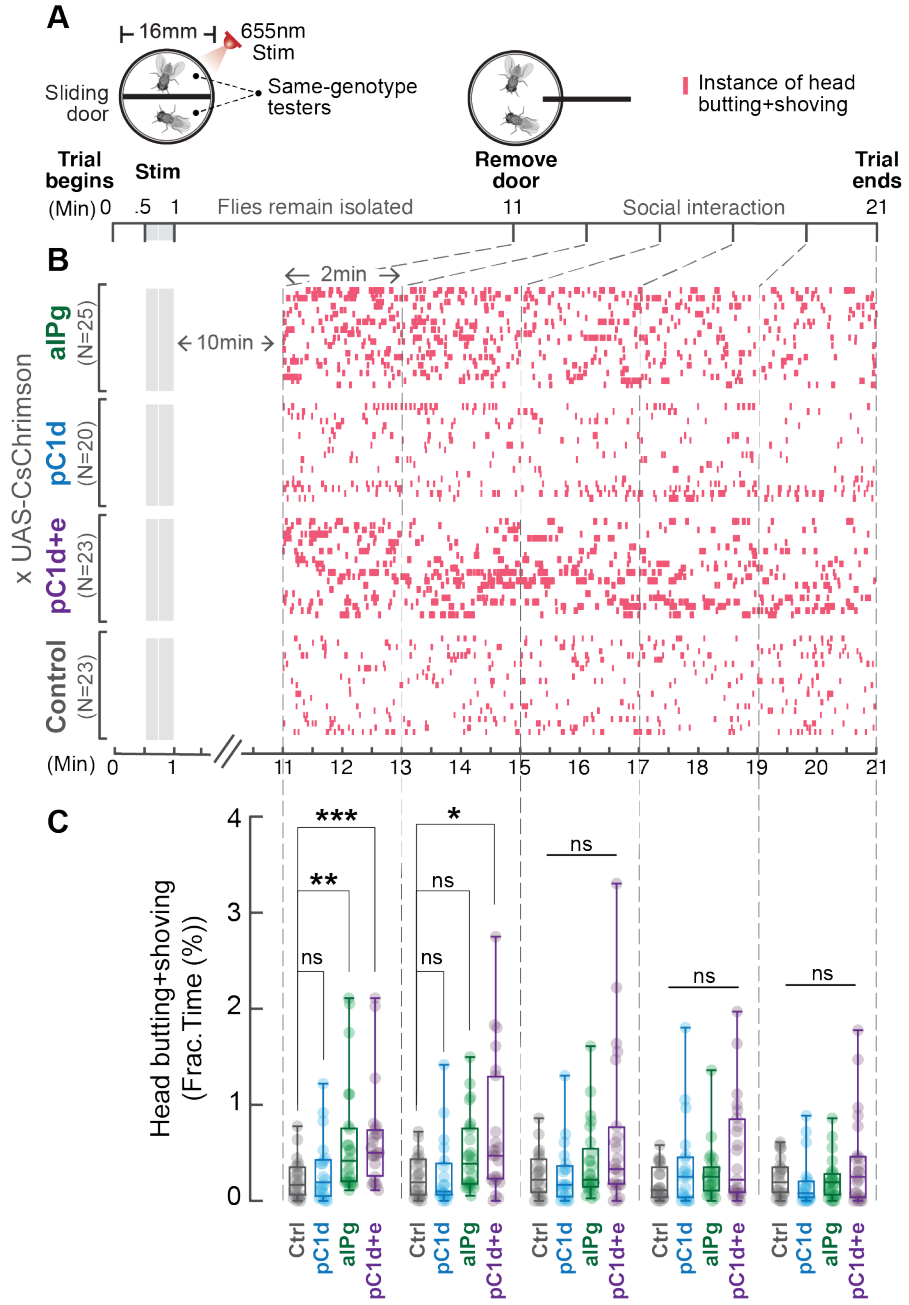

Fig. 2. Brief stimulation of aIPg, but not pC1d alone promotes persistent female aggression. Cell-specific contributions of aIPg, pC1d, and pC1d+e neurons to persistent aggressive internal state were tested using the sliding door assay (A). Same-genotype testers were separated by a sliding door in the behavioral chamber while receiving a brief 655 nm light stimulation (13+15 seconds). Doors were removed 10 minutes after the stimulation to allow the flies to interact. Level of female aggression (head butting + shoving, red ticks) is shown in the raster plot (B). Fraction of time spent on fighting by each genotype female is compared in the box plot (C). Data were combined from three independent biological repeats. ***p<0.001; **p<0.01; *p<0.05; ns, not significant. Control, empty split-Gal4 driver (BDP-AD; BDP-DBD).

increase aggression during or following stimulation (data not shown), as previously reported (2). The aIPg-induced persistent aggression lasted minutes in this paradigm, which is longer than the tens of seconds-long persistence we reported previously (2). As there is a 7-fold difference in the fly density per area in the two experiments (current study: 0.2 flies per sq. cm; Schretter et al. (2020): 0.03 flies per sq. cm) and since density is known to alter social behaviors (24), we asked if the duration of persistence was influenced by the fly density in the chamber. Indeed, we found that even a modest increase in fly density (0.08 flies per sq. cm) extended persistent aggression in both aIPg and pC1d+e activated flies. These observations suggest that the frequency of social encounters can be an external factor that increases the duration of aggression (Supplementary Figure 4).

pC1d-aIPg functional connectivity is not required for aIPg-induced persistent aggression. We investigated whether the reciprocal pC1d-aIPg connectivity (Figure 1A) is required for aIPg-induced persistent aggression by perform-

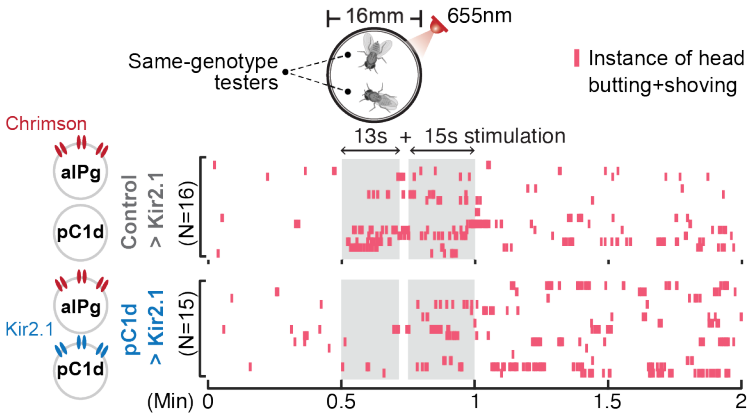

Fig. 3. pC1d-aIPg recurrent connectivity is not required for aIPg-induced persistent aggressive behavior. Inhibition of pC1d by Kir2.1 expression did not suppress aIPg-induced persistent aggression. Aggression (head butting+shoving, red ticks) is shown in the raster plot. Flies were freely interacting throughout the experiments, and the data were combined from two independent biological repeats. The differences between Control > Kir2.1 and pC1d > Kir2.1 groups in the separate 13s and 15s stimulation periods were not significant (13s period, p = 0.2978; 15s period, p = 0.6650). See Supplementary Figure 5 for quantification. Control, empty split-Gal4 driver (BDP-AD; BDP-DBD).

ing behavioral epistasis and *in vivo* calcium imaging experiments. Using the expression of the inwardly rectifying potassium channel Kir2.1 (25), we inhibited the activity of pC1d neurons while aIPg neurons were activated for 30 seconds in freely interacting females (Figure 3 and Supplementary Figure 5). As aIPg-induced persistent aggression was found in the same genotype (2) and mixed pair assays (Supplementary Figure 3), we used the same genotype pairs to investigate if pC1d inactivation altered aIPg-induced behavior. Surprisingly, chronic inhibition of pC1d neurons did not suppress aggression after aIPg stimulation, suggesting that feedback from pC1d neurons is not necessary for the persistent aggressive state promoted by aIPg neurons (Figure 3 and Supplementary Figure 5).

We next turned to *in vivo* imaging experiments to examine whether pC1d or aIPg neurons themselves exhibit persistent activity, and if so whether the strong recurrent connections between these cholinergic cells (20) contributes to such persistence. To evaluate the role of these connections, we applied either a short (5 Hz, 30 second) stimulus, as used in our current behavioral assays, or a long (50 Hz, 300 second) stimulus (as used in (1)) to activate aIPg or pC1d neurons while simultaneously imaging calcium transients in either cell type using GCaMP, in head-fixed females under a two-photon microscope (Figure 4 and Supplementary Figure 6).

We found that neither short (30 second) (Figure 4C-D) nor long (300 second) (Supplementary Figure 6C-D) stimulation of aIPg neurons triggered persistent activity in pC1d neurons or vice versa. Because aIPg neurons form reciprocal connections amongst themselves (Figure 1A), we also examined whether direct stimulation of aIPg neurons could cause persistent activity in these cells. We found that the response of aIPg neurons was time-locked to the stimulation period regardless of stimulation length (Figure 4B and Supplementary Figure 6B). Given that a 30 second stimulation of aIPg neurons in intact flies is sufficient to elicit a persistent aggressive state that lasts longer than 10 minutes, it seems that neither aIPg nor pC1d neurons exhibit persistent activity on the time scale necessary to sustain persistent aggressive behavior. Together, our behavioral epistasis and *in vivo* imaging data indicate that reciprocal connections among aIPg neurons or between pC1d and aIPg neurons are neither required nor sufficient to generate a persistent internal state of aggressiveness. Therefore, persistent aggressive behavior is likely regulated by other downstream neurons that transform the output of aIPg or pC1d+e neurons.

Concluding Remarks

This work demonstrates that optogenetic stimulation of aIPg neurons at the same levels needed to produce aggression during photo-stimulation also promoted a minutes-long behaviorally latent, persistent internal state of aggressiveness (or social arousal). In contrast, pC1d neuronal stimulation with the same optogenetic parameters generated time-locked aggression but not a latent, persistent internal state. However, such a persistent internal state was observed when pC1d and pC1e were co-stimulated. Our epistasis experiments do not support a model in which persistent aggression in females is driven by pC1d neurons acting through recurrent connections with aIPg neurons. Our imaging data further indicate that neither aIPg nor pC1d neurons themselves exhibit persistent neural activity when directly or indirectly stimulated, raising the question of how the persistent aggressive state is sustained by the downstream targets of these neurons and what role pC1e plays.

Our connectomic analysis revealed that aIPg, pC1d, and pC1e neurons have both unique and shared downstream targets (Supplementary Figure 2). pC1d and pC1e neurons form a relatively small number of synapses with one another (Figure 1A and Supplementary Figure 2A); however, aIPg neurons form strong reciprocal connections with both pC1d and pC1e as well as among themselves. While aIPg neurons' recurrent synapses within the neuronal subset was a candidate for maintaining persistence, the GCaMP signals in aIPg were time-locked to the stimulus when aIPg neurons were acti-

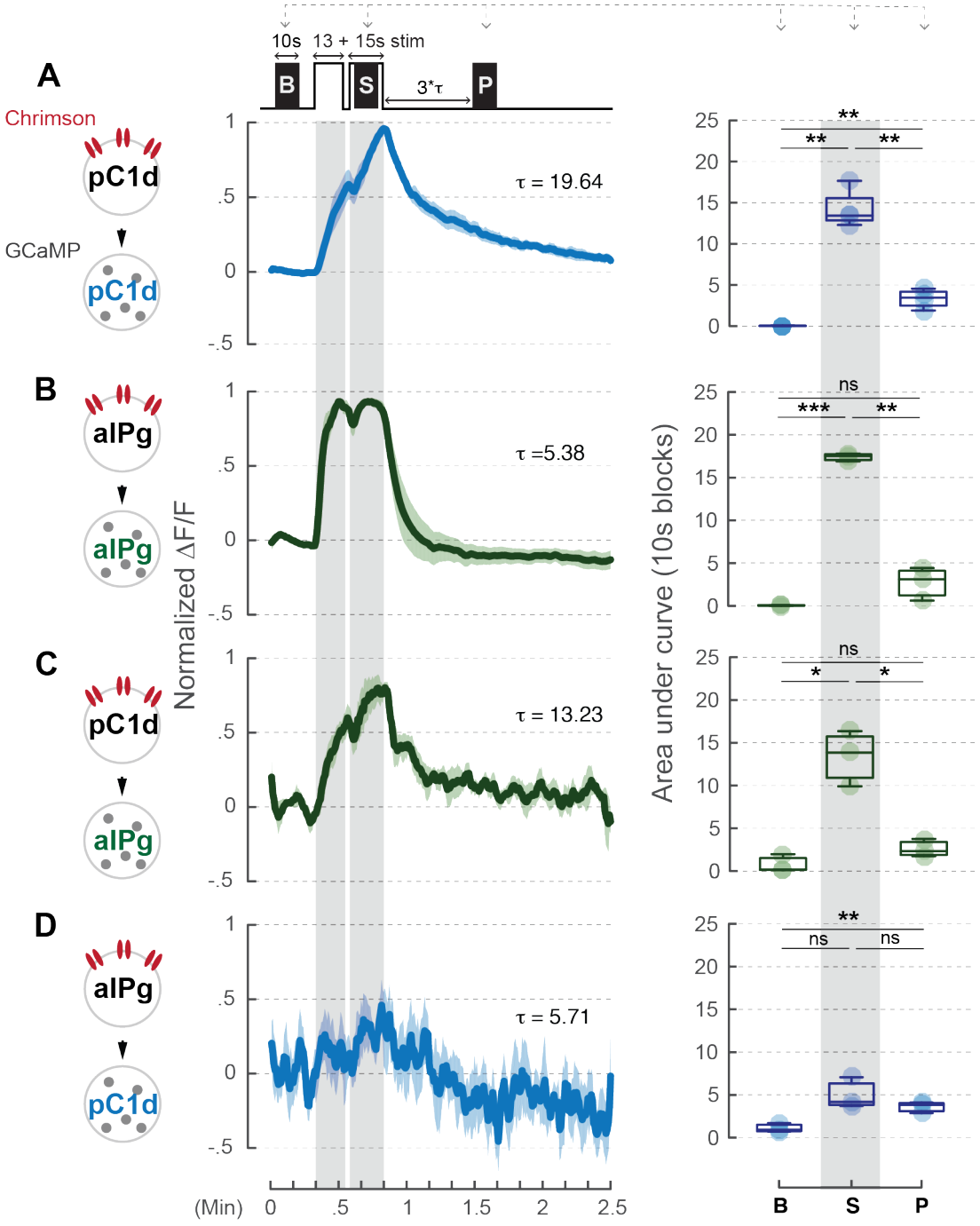

Fig. 4. Neural activity of aIPg neurons is not prolonged by pC1d-aIPg or aIPg-aIPg recurrent connectivity. A brief 660 nm stimulation that mimics the one used in the behavioral experiment was applied to activate the Chrimson-expressing neurons: pC1d (A or C) and aIPg (B or D). GCaMP responses of pC1d (A or D) or aIPg (B or C) neurons are shown by the blue and green traces, respectively. Dark blue/green line, mean. Light blue/green line, SEM. Tau of GCaMP signals in pC1d neurons is 19.64 seconds and 5.71 seconds when pC1d or aIPg neurons were stimulated, respectively. Tau of GCaMP signals in aIPg neurons is 5.38 seconds and 13.23 seconds when aIPg or pC1d neurons were stimulated, respectively. Area under the GCaMP trace during the 10 second blocks in the baseline (B), stimulation (S), and post-stimulation (P; measured at 3 times Tau after stimulation) period were compared in the box plots shown at right of panel. The difference between B and P in (D) was not significant after multiple comparisons correction. Data were combined from three to four independent biological repeats. Light blue/green circle, individual data. ***p<0.001; **p<0.01; *p<0.05; ns, not significant.

vated. Additionally, pC1d stimulation triggered only time-locked responses in aIPg neurons (Figure 4).

The results reported here confirm the observation of (1) that co-stimulation of pC1d and pC1e promotes persistent aggression, but reveal paradoxically that stimulation of pC1d alone promotes only time-locked, but not persistent aggression. Given that stimulation of aIPg alone can promote persistent aggression in the absence of pC1d activity, these results provide evidence of distinct classes of neurons controlling aggression in a time-locked versus persistent manner. The biological significance of this distinction remains to be determined. Additionally, our data reveal a key role for pC1e in maintaining persistent aggression, despite the fact that these neurons do not produce aggression when optogenetically stimulated alone. This observation suggests that persistent aggression promoted by pC1d+e is an emergent property of their co-activation. We note that pC1e receives distinct inputs that possibly indicate the presence of another fly (Supplementary Figure 2). While pC1e also forms recurrent connections with aIPg, these synapses constitute a relatively low proportion of the total output of aIPg (0.177%). Interestingly, the function of pC1e neurons resembles that of pCd neurons in males, in that both classes of neurons regulate the persistence of internal states but do not directly evoke aggressive behavior when stimulated (6). However, pCd neurons are a cell type distinct from pC1d and pC1e neurons.

This study focused on the cell type-specific contribution of aIPg, pC1d, and pC1e neurons as well as the role of their recurrent connectivity. The persistence of aggressive states could be regulated by additional circuit components not present in our driver lines or other mechanisms, including neuropeptide modulation or prior experience (16, 26, 27). Identifying such components and their mechanisms of action will be an important focus for future work. RNA profiling data indicate that aIPg neurons produce the neuropeptide sNPF (2) and downstream targets might produce additional neuropeptides. Neuropeptides can act over the timescales needed to generate persistent aggressive behavior (4). Additional mechanisms include attractor dynamics as suggested by a recent study in mice (28). How neural circuits implement a persistent aggressive state, and whether individual circuit elements control distinct features of the aggressive state, remain major open questions that can be addressed by future studies of this circuit.

Methods and Materials

Fly strains. Please see supplementary file 1 for full genotypes of flies used in each figure and sources of flies. Briefly, the cell type-specific drivers were generated at Janelia Research Campus and the split-GAL4 drivers were previously reported in Schretter et al. (2020). Depending on the experiments, the aIPg neurons were labeled by aIPg-SS (SS36565; VT064565-p65ADZp(attP40); VT043699-ZpGDBD(attP2)) or 72C11-LexA (attp-40). Drivers for the pC1d or pC1d+e neurons were pC1d-SS (SS56987; 35C10-p65ADZp(JK73A); 71A09-ZpGDBD(attP2)) and pC1d+e-SS (SS43274; VT025602-p65ADZp (attP40); VT002064-ZpGDBD (attP2)/TM6B), respectively. Canton-S was used as wild-type target flies in mixed pair experiments. 72C11LexA (attp40), 13xLexAop2-CsChrimson::tdT3.1 (su(Hw)attp5); 10xUAS-eGFP::Kir2.1(attp2) used in the behavioral epistasis experiment was generated in the Anderson lab.

Rearing conditions. Stocks and crosses were reared at 25°C and 50% humidity and maintained on a 12hr:12hr light:dark cycle. Fly density was kept consistent across experiments by crossing 10-12 virgin females with 5-6 males and flipping every two days. Experimental flies were collected as virgins and group housed (approx. 20 flies per vial) on vials containing retinal food (0.2 mM) in the dark. Flies were flipped into fresh vials containing food one day before behavioral testing.

Behavioral Assays. Unless otherwise stated, the behavioral chambers used were 6 mm-high 16 mm-diameter acrylic cylinders with a clear top and floor. The wall and lids were coated with Insect-A-Slip and silicon fluid, respectively. The floor was covered with freshly prepared apple juice agar (2.5% (w/v) sucrose and 2.25% (w/v) agarose in apple juice) and illuminated with an 850 nm backlight (SOBL-200x150-850, SmartVision Lights, Muskegon, MI). Flies were introduced into the chambers by gentle aspiration and allowed to settle for at least 2 minutes prior to testing. Behaviors were recorded from above using a Point Grey Flea3 camera recording at 30 fps using a long pass IR filter (780 nm, Midwest Optical Systems). Flies were tested during the evening peak (Zeitgeber (ZT) 9 – 12).

Sliding door assay. Detailed descriptions of the behavioral setup can be found in (29) and (19). Briefly, sliding door experiments were performed in identical arenas apart from a vertical barrier that divides each chamber in half. Females were loaded into separate sides of the barrier and allowed to acclimate for 2 minutes before recording. Each trial comprised of the pre-stimulation (30 second), stimulation (30 second), post-stimulation I (600 second), buffering (10 second), and post-stimulation II (600 second) period. The stimulation period comprises two stimulation blocks (13 and 15 seconds) separated by a 2 second inter-stimulation interval. For each stimulation block, a 655 nm LED above each chamber delivers 5 Hz pulsed light with a maximum intensity of 0.62 μW/mm^2. Barriers were manually removed during the buffering period, meaning that social interaction is only allowed 10 minutes after neural stimulation. Interaction during the buffering period was not tracked due to the movement of the barrier. Please see Behavioral analysis for quantification of aggressive behavior.

Mixed-pair assay. To distinguish target versus tester in each experimental pair, one wing of the group housed Canton-S target is cut shorter one day before the experiment. Flies interacted freely in the chamber during the entire trial. Each trial comprised of the pre-stimulation (30 second), stimulation (30 second), and post-stimulation (120 second) period. The stimulation condition is the same as the sliding door assay. Please see Behavioral analysis for quantification of aggressive behavior.

Table 1. Head butting and shoving JAABA classifier.

Classifier	True Positive	True Negative	False Positive	False Negative
Head butting+shoving	80% (204)	83.3% (1957)	20% (51)	16.7% (392)

Density experiment. 15 or 40 group housed mated female flies were introduced via gentle aspiration into a 127 mm diameter arena as described in (2). Flies were tested during the morning peak (ZT 0 – 3) to replicate the conditions from (2). The arena received was performed under white light illumination from above. Flies were acclimatized to the arena for 30 seconds prior to delivery of a single constant stimulus (1 mW/cm^2) from below with 660 nm LEDs lasting 30 seconds. Videos in this setup were recorded from above using a Point Grey Flea3 camera with an 800 nm long pass filter (B and W filter; Schneider Optics, Hauppauge, NY) at 30 fps.

Behavior analysis. Flies were tracked using the Caltech FlyTracker (http://www.vision.caltech.edu/Tools/FlyTracker/) followed by automated classification of behavior with a JAABA classifier for head butting and shoving behaviors (see Table 1; 80% (true positive) and 83.3% (true negative) framewise performance). Due to the camera resolution, head butting could not be distinguished from shoving and an instance of head butting and shoving was defined as when a fly moved towards the other, thrusting its head or forelimbs towards the other fly. All behavioral bouts were manually curated using the Caltech FlyTracker Visualizer to eliminate false positives and false negatives. Calculations of the fraction of time spent performing a behavior were made using the score files and averaging over the period indicated. To separate out the wild-type (Canton-S) target from the genotype of interest, mixed pair experiments were manually corrected for tracking errors using the FixErrors Matlab GUI (https://ctrax.sourceforge.net/fixerrors.html). For density experiments, the same classifier used in (2) was employed.

In vivo calcium imaging. Experiments were performed as detailed in (22). Briefly, six-day-old experimental flies were anesthetized on ice and head-fixed with the UV glue in their normal standing posture. The top of the fly head was immersed in fly saline, and a piece of cuticle (350 μm by 350 μm) was removed from the posterior side of the head capsule to create an imaging window. After surgery, the experimental fly was placed under a 0.8 numerical aperture (NA) 40x objective (LUMPLFLN40XW, Olympus) and habituated for at least 5 minutes. The optical setup for two-photon imaging with optogenetic activation was described in (29). Two stimulation paradigms were used: 13 and 15 second 5 Hz stimulation with 2 second inter-stimulation interval (same as the behavioral assays) or 5 minute 50 Hz stimulation (for replicating the stimulation used in (1)). To calculate the decay time constant (Tau τ), we fitted the GCaMP signals (a 15-second window that immediately follows the stimulation) with a one-term exponential model (MATLAB toolbox, function 'fit'). Tau is calculated as -1/b.

Connectomic analysis. The primary data used for our analyses are described in (20). Hemibrain data was queried using NeuPrint and v1.2.1 of the connectome (neuprint.janelia.org). Cytoscape (cytoscape.org) was used to produce the node layout of connectivity diagrams of connections between neurons, which were then edited in Adobe Illustrator. Thresholds were used to limit the number of neurons in the figures to those connections with the most synapses. For Supplementary Figure 2, a threshold of 25 synapses between types was used, except for the connections from pC1d and pC1e in which all synapses were shown. In all cases, a threshold of three synapses was applied to connections between individual cells. Higher specific thresholds, when applied, are specified in each figure legend. A complete list of synaptic connections can be found in NeuPrint.

Statistics and quantification. No statistical methods were used to pre-determine sample size. Sample size was based on previous literature in the field and experimenters were not blinded in most conditions as almost all data acquisition and analysis were automated. Biological replicates completed at separate times using different parental crosses were performed for each of the behavioral experiments. For mixed pair and sliding door experiments, three biological repeats were performed, and the data was combined. For density experiments, data is representative of two independent biological repeats, only one of which is shown. For figures in which the behavioral data over the course of a trial is shown, grey shading indicates the stimulus period, the mean is represented as a solid line, and shaded error bars represent variation between experiments. For raster plots, each red line represents a bout in which either individual in the arena displayed head butting or shoving behavior. In the mixed pair experiments, data from the wild-type target was not included.

For each experiment, the experimental and control flies were collected, treated and tested at the same time. A Kruskal-Wallis test and Dunn's post hoc test was used for statistical analysis for behavioral experiments. For Figure 4 and Supplementary Figure 6, a paired-t test was used for statistical analysis. All statistical analysis was performed using Prism Software (GraphPad, version 9). p values are indicated as follows: ****p<0.0001; ***p<0.001; **p<0.01; and *p<0.05. See supplementary file 1 for exact p-values for each figure.

Boxplots show median and interquartile range (IQR). Lower and upper whiskers represent 1.5 × IQR of the lower and upper quartiles, respectively; boxes indicate lower quartile, median, and upper quartile, from bottom to top. When all points are shown, whiskers represent range and boxes indicate lower quartile, median, and upper quartile, from bottom to top. Shaded error bars on graphs are presented as mean ± s.e.m.

ACKNOWLEDGEMENTS

We thank M. Dreher (Dreher Design Studio) for help with connectomics figures; A. Sanchez (Caltech) for fly maintenance; C. Chiu, G. Mancuso, L. Chavarria, X. Da (Caltech), and A. Howard (Janelia) for laboratory management and administrative assistance; and Dr. D. Bushey (Janelia) for help with additional calcium imaging

experiments. We also thank Drs. D. Deutsch, U. Heberlein, M. Murthy, and A. Otopalik for their helpful feedback on the manuscript as well as the broader Janelia community for their suggestions throughout this work.

Bibliography

1. David Deutsch, Diego Pacheco, Lucas Encarnacion-Rivera, Talmo Pereira, Ramie Fathy, Jan Clemens, Cyrille Girardin, Adam Calhoun, Elise Ireland, Austin Burke, Sven Dorkenwald, Claire McKellar, Thomas Macrina, Ran Lu, Kisuk Lee, Nico Kemnitz, Dodam Ih, Manuel Castro, Akhilesh Halageri, Chris Jordan, William Silversmith, Jingpeng Wu, H Sebastian Seung, and Mala Murthy. The neural basis for a persistent internal state in Drosophila females. *eLife*, 9:e59502, November 2020. ISSN 2050-084X. doi: 10.7554/eLife.59502.
2. Catherine E Schretter, Yoshinori Aso, Alice A Robie, Marisa Dreher, Michael-John Dolan, Nan Chen, Masayoshi Ito, Tansy Yang, Ruchi Parekh, Kristin M Branson, and Gerald M Rubin. Cell types and neuronal circuitry underlying female aggression in Drosophila. *eLife*, 9:e58942, November 2020. ISSN 2050-084X. doi: 10.7554/eLife.58942.
3. David J. Anderson and Ralph Adolphs. A framework for studying emotions across species. *Cell*, 157(1):187–200, March 2014. ISSN 0092-8674, 1097-4172. doi: 10.1016/j.cell.2014.03.003.
4. Steven W. Flavell, Nadine Gogolla, Matthew Lovett-Barron, and Moriel Zelikowsky. The emergence and influence of internal states. *Neuron*, 110:2545–2570, August 2022. ISSN 08966273. doi: 10.1016/j.neuron.2022.04.030.
5. Steven W. Flavell, Navin Pokala, Evan Z. Macosko, Dirk R. Albrecht, Johannes Larsch, and Cornelia I. Bargmann. Serotonin and the neuropeptide PDF initiate and extend opposing behavioral states in C. elegans. *Cell*, 154(5):1023–1035, August 2013. ISSN 0092-8674. doi: 10.1016/j.cell.2013.08.001.
6. Yonil Jung, Ann Kennedy, Hui Chiu, Farhan Mohammad, Adam Claridge-Chang, and David J. Anderson. Neurons that function within an integrator to promote a persistent behavioral state in Drosophila. *Neuron*, 105(2):322–333.e5, January 2020. ISSN 0896-6273. doi: 10.1016/j.neuron.2019.10.028.
7. Ann Kennedy, Prabhat S. Kunwar, Ling-yun Li, Stefanos Stagkourakis, Daniel A. Wagenaar, and David J. Anderson. Stimulus-specific hypothalamic encoding of a persistent defensive state. *Nature*, 586(7831):730–734, October 2020. ISSN 1476-4687. doi: 10.1038/s41586-020-2728-4.
8. João C. Marques, Meng Li, Diane Schaak, Drew N. Robson, and Jennifer M. Li. Internal state dynamics shape brainwide activity and foraging behaviour. *Nature*, 577(7789):239–243, January 2020. ISSN 1476-4687. doi: 10.1038/s41586-019-1858-z.
9. Jeffrey L. Rhoades, Jessica C. Nelson, Ijeoma Nwabudike, Stephanie K. Yu, Ian G. McLachlan, Gurrein K. Madan, Eden Abebe, Joshua R. Powers, Daniel A. Colón-Ramos, and Steven W. Flavell. ASICs mediate food responses in an enteric serotonergic neuron that controls foraging behaviors. *Cell*, 176(1):85–97.e14, January 2019. ISSN 0092-8674, 1097-4172. doi: 10.1016/j.cell.2018.11.023.
10. Drew N. Robson and Jennifer M. Li. A dynamical systems view of neuroethology: Uncovering stateful computation in natural behaviors. *Current Opinion in Neurobiology*, 73:102517, April 2022. ISSN 0959-4388. doi: 10.1016/j.conb.2022.01.002.
11. Stephen X. Zhang, Andrew Lutas, Shang Yang, Adriana Diaz, Hugo Fluhr, Georg Nagel, Shiqiang Gao, and Mark L. Andermann. Hypothalamic dopamine neurons motivate mating through persistent cAMP signalling. *Nature*, 597(7875):245–249, September 2021. ISSN 1476-4687. doi: 10.1038/s41586-021-03845-0.
12. Zengcai V. Guo, Hidehiko K. Inagaki, Kayvon Daie, Shaul Druckmann, Charles R. Gerfen, and Karel Svoboda. Maintenance of persistent activity in a frontal thalamocortical loop. *Nature*, 545(7653):181–186, May 2017. ISSN 1476-4687. doi: 10.1038/nature22324.
13. Hidehiko K. Inagaki, Lorenzo Fontolan, Sandro Romani, and Karel Svoboda. Discrete attractor dynamics underlies persistent activity in the frontal cortex. *Nature*, 566(7743):212–217, February 2019. ISSN 1476-4687. doi: 10.1038/s41586-019-0919-7.
14. David A. McCormick. Brain calculus: neural integration and persistent activity. *Nature Neuroscience*, 4(2):113–114, February 2001. ISSN 1546-1726. doi: 10.1038/83917.
15. Xiao-Jing Wang. Synaptic reverberation underlying mnemonic persistent activity. *Trends in Neurosciences*, 24(8):455–463, August 2001. ISSN 0166-2236. doi: 10.1016/S0166-2236(00)01868-3.
16. Eartha Mae Guthman and Annegret L. Falkner. Neural mechanisms of persistent aggression. *Current Opinion in Neurobiology*, 73:102526, April 2022. ISSN 0959-4388. doi: 10.1016/j.conb.2022.102526.
17. Eric D Hoopfer. Neural control of aggression in Drosophila. *Current Opinion in Neurobiology*, 38:109–118, June 2016. ISSN 0959-4388. doi: 10.1016/j.conb.2016.04.007.
18. Edward A. Kravitz and Maria de la Paz Fernandez. Aggression in Drosophila. *Behavioral Neuroscience*, 129(5):549–563, October 2015. ISSN 1939-0084. doi: 10.1037/bne0000089.
19. Eric D Hoopfer, Yonil Jung, Hidehiko K Inagaki, Gerald M Rubin, and David J Anderson. P1 interneurons promote a persistent internal state that enhances inter-male aggression in Drosophila. *eLife*, 4:e11346, December 2015. ISSN 2050-084X. doi: 10.7554/eLife.11346.
20. Louis K Scheffer, C Shan Xu, Michal Januszewski, Zhiyuan Lu, Shin-ya Takemura, Kenneth J Hayworth, Gary B Huang, Kazunori Shinomiya, Jeremy Maitlin-Shepard, Stuart Berg, Jody Clements, Philip M Hubbard, William T Katz, Lowell Umayam, Ting Zhao, David Ackerman, Tim Blakely, John Bogovic, Tom Dolafi, Dagmar Kainmueller, Takashi Kawase, Khaled A Khairy, Laramie Leavitt, Peter H Li, Larry Lindsey, Nicole Neubarth, Donald J Olbris, Hideo Otsuna, Eric T Trautman, Masayoshi Ito, Alexander S Bates, Jens Goldammer, Tanya Wolff, Robert Svirskas, Philipp Schlegel, Erika Neace, Christopher J Knecht, Chelsea X Alvarado, Dennis A Bailey, Samantha Ballinger, Jolanta A Borycz, Brandon S Canino, Natasha Cheatham, Michael Cook, Marisa Dreher, Octave Duclos, Bryon Eubanks, Kelli Fairbanks, Samantha Finley, Nora Forknall, Audrey Francis, Gary Patrick Hopkins, Emily M Joyce, SungJin Kim, Nicole A Kirk, Julie Kovalyak, Shirley A Lauchie, Alanna Lohff, Charli Maldonado, Emily A Manley, Sari McLin, Caroline Mooney, Miatta Ndama, Omotara Ogundeyi, Nneoma Okeoma, Christopher Ordish, Nicholas Padilla, Christopher M Patrick, Tyler Paterson, Elliott E Phillips, Emily M Phillips, Neha Rampally, Caitlin Ribeiro, Madelaine K Robertson, Jon Thomson Rymer, Sean M Ryan, Megan Sammons, Anne K Scott, Ashley L Scott, Aya Shinomiya, Claire Smith, Kelsey Smith, Natalie L Smith, Margaret A Sobeski, Alia Suleiman, Jackie Swift, Satoko Takemura, Iris Talebi, Dorota Tarnogorska, Emily Tenshaw, Temour Tokhi, John J Walsh, Tansy Yang, Jane Anne Horne, Feng Li, Ruchi Parekh, Patricia K Rivlin, Vivek Jayaraman, Marta Costa, Gregory SXE Jefferis, Kei Ito, Stephan Saalfeld, Reed George, Ian A Meinertzhagen, Gerald M Rubin, Harald F Hess, Viren Jain, and Stephen M Plaza. A connectome and analysis of the adult Drosophila central brain. *eLife*, 9:e57443, September 2020. ISSN 2050-084X. doi: 10.7554/eLife.57443.
21. Kenta Asahina. Neuromodulation and strategic action choice in Drosophila aggression. *Annual Review of Neuroscience*, 40:51–75, July 2017. ISSN 1545-4126. doi: 10.1146/annurev-neuro-072116-031240.
22. Hui Chiu, Eric D. Hoopfer, Maeve L. Coughlan, Hania J. Pavlou, Stephen F. Goodwin, and David J. Anderson. A circuit logic for sexually shared and dimorphic aggressive behaviors in Drosophila. *Cell*, 184(2):507–520.e16, January 2021. ISSN 1097-4172. doi: 10.1016/j.cell.2020.11.048.
23. Caroline B. Palavicino-Maggio, Yick-Bun Chan, Claire McKellar, and Edward A. Kravitz. A small number of cholinergic neurons mediate hyperaggression in female Drosophila. *Proceedings of the National Academy of Sciences of the United States of America*, 116(34):17029–17038, August 2019. ISSN 1091-6490. doi: 10.1073/pnas.1907042116.
24. Rebecca Rooke, Amara Rasool, Jonathan Schneider, and Joel D. Levine. Drosophila melanogaster behaviour changes in different social environments based on group size and density. *Communications Biology*, 3(1):1–6, June 2020. ISSN 2399-3642. doi: 10.1038/s42003-020-1024-z.
25. Richard A. Baines, Jay P. Uhler, Annemarie Thompson, Sean T. Sweeney, and Michael Bate. Altered electrical properties in Drosophila neurons developing without synaptic transmission. *The Journal of Neuroscience*, 21:1523–1531, March 2001. ISSN 0270-6474, 1529-2401. doi: 10.1523/JNEUROSCI.21-05-01523.2001.
26. Ann Kennedy. The what, how, and why of naturalistic behavior. *Current Opinion in Neurobiology*, 74:102549, June 2022. ISSN 0959-4388. doi: 10.1016/j.conb.2022.102549.
27. Guy Major and David Tank. Persistent neural activity: prevalence and mechanisms. *Current Opinion in Neurobiology*, 14(6):675–684, December 2004. ISSN 0959-4388. doi: 10.1016/j.conb.2004.10.017.
28. Aditya Nair, Tomomi Karigo, Bin Yang, Surya Ganguli, Mark J. Schnitzer, Scott W. Linderman, David J. Anderson, and Ann Kennedy. An approximate line attractor in the hypothalamus encodes an aggressive state. *Cell*, 186(1):178–193.e15, January 2023. ISSN 0092-8674. doi: 10.1016/j.cell.2022.11.027.
29. Hidehiko K. Inagaki, Yonil Jung, Eric D. Hoopfer, Allan M. Wong, Neeli Mishra, John Y. Lin, Roger Y. Tsien, and David J. Anderson. Optogenetic control of Drosophila using a red-shifted channelrhodopsin reveals experience-dependent influences on courtship. *Nature Methods*, 11(3):325–332, March 2014. ISSN 1548-7105. doi: 10.1038/nmeth.2765.
30. Nils Eckstein, Alexander S. Bates, Michelle Du, Volker Hartenstein, Gregory S. X. E. Jefferis, and Jan Funke. Neurotransmitter classification from electron microscopy images at synaptic sites in Drosophila, September 2020.
31. Ming Wu, Aljoscha Nern, W Ryan Williamson, Mai M Morimoto, Michael B Reiser, Gwyneth M Card, and Gerald M Rubin. Visual projection neurons in the Drosophila lobula link feature detection to distinct behavioral programs. *eLife*, 5:e21022, December 2016. ISSN 2050-084X. doi: 10.7554/eLife.21022.
32. Inês M. A. Ribeiro, Michael Drews, Armin Bahl, Christian Machacek, Alexander Borst, and Barry J. Dickson. Visual projection neurons mediating directed courtship in Drosophila. *Cell*, 174(3):607–621.e18, July 2018. ISSN 1097-4172. doi: 10.1016/j.cell.2018.06.020.

Experimental paradigms used in Schretter et al. (2020) vs. Deutsch et al. (2020).

		Schretter et al. (2020)				Deutsch et al. (2020)			
Behavior	Stimulated neurons	aIPg	pC1d	pC1e	pC1d+e (pC1-A)	aIPg	pC1d	pC1e	pC1d+e (pC1-A)
	Tester	♀	♀	♀	♀	--	--	--	♀
	Target	♀	♀	♀	♀	--	--	--	♂
	Stimulation Condition	30s 617nm	30s 617nm	30s 617nm	30s 617nm	--	--	--	up to 5min* 627nm
	Aggression during stim	Yes	Yes	No	Yes	--	--	--	-- **
	Persistant aggression	Yes	No	No	Yes #	--	--	--	Yes
	Effector	CsChR	CsChR	CsChR	CsChR	--	--	--	ReachR
Imaging	Stimulated neurons	--	--	--	--	--	--	--	pC1d+e (pC1-A)
	Recorded neurons	--	--	--	--	--	--	--	*dsx+* and *fru+* neurons ***
	Stimulation Condition	--	--	--	--	--	--	--	up to 5min* 700nm
	Persistant activity	--	--	--	--	--	--	--	Yes

* The authors tested 30 sec, 2 min, and 5 min protocols and observed significant persistent behavior following 2 min and 5 min conditions.

** Interaction was prevented during stimulation.

*** Cell identity is inferred by the cell body location and includes pC1 and aIPg neurons.

\# Duration is very brief

-- Did not test

Fig. S1. Comparison of the experimental designs used in Schretter et al. (2020) and Deutsch et al. (2020) Experimental conditions and results of the behavioral and imaging experiments demonstrated in Schretter et al. (2020) and Deutsch et al. (2020) are compared. For behavioral experiments, the major differences between the two papers are in the stimulation duration (30 seconds vs. up to 5 minutes), gender of the target (female vs. male), and optogenetic effector (CsChrimson vs. ReachR). Based on the cell body location in pan-neuronal GCaMP imaging, (1) conclude that persistent activity was observed in pC1 and aIPg neurons.

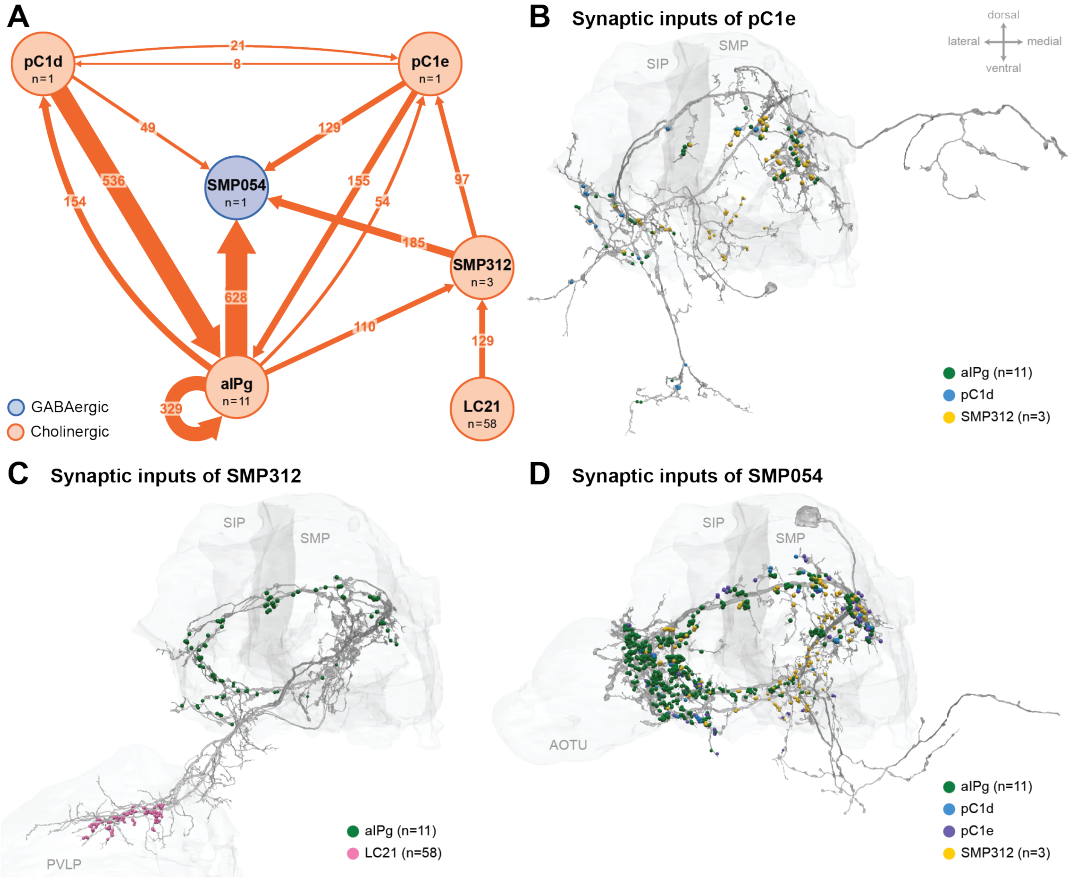

Fig. S2. Additional circuit components. Common prominent targets and inputs to aIPg, pC1d, and pC1e neurons. (A) aIPg neurons form direct and indirect connections with pC1e. The most prominent indirect connection goes through the interneuron SMP312. Previous connectomic analysis highlighted SMP054 neurons in a circuit indirectly linking aIPg with LC10 neurons, a specific type of lobula columnar visual output neurons tuned to small moving objects (2, 31, 32). In addition to being common target of aIPg, pC1d, and pC1e, SMP054 receives indirect visual input through SMP312 possibly indicating the presence of another fly. Because our attempts to generate cell-type-specific driver lines for SMP054 have failed, we cannot test the behavior generated by SMP054 activation. Synapse number is noted on each arrow and neurotransmitter predictions (30) are indicated by color (blue, GABAergic; orange, cholinergic). A threshold of 25 synapses was applied, except for the connectivity between pC1d and pC1e. (B) Distribution of synaptic inputs from aIPg (green), pC1d (blue), and SMP312 (yellow) on the neuronal skeleton of pC1e. (C) Distribution of synaptic inputs from aIPg (green) and LC21 (pink) on the neuronal skeleton of SMP312. (D) Distribution of synaptic inputs from aIPg (green), pC1d (blue), pC1e (purple), and SMP312 (yellow) on the neuronal skeleton of SMP054. Select brain regions (SIP, superior intermediate protocerebrum; SMP, superior medial protocerebrum; PVLP, posterior ventrolateral protocerebrum; AOTU, anterior optic tubercle) are outlined in light grey. Dorsal side of the model brain is up, and the lateral is towards the left. Data are from NeuPrint hemibrain v1.2.1.

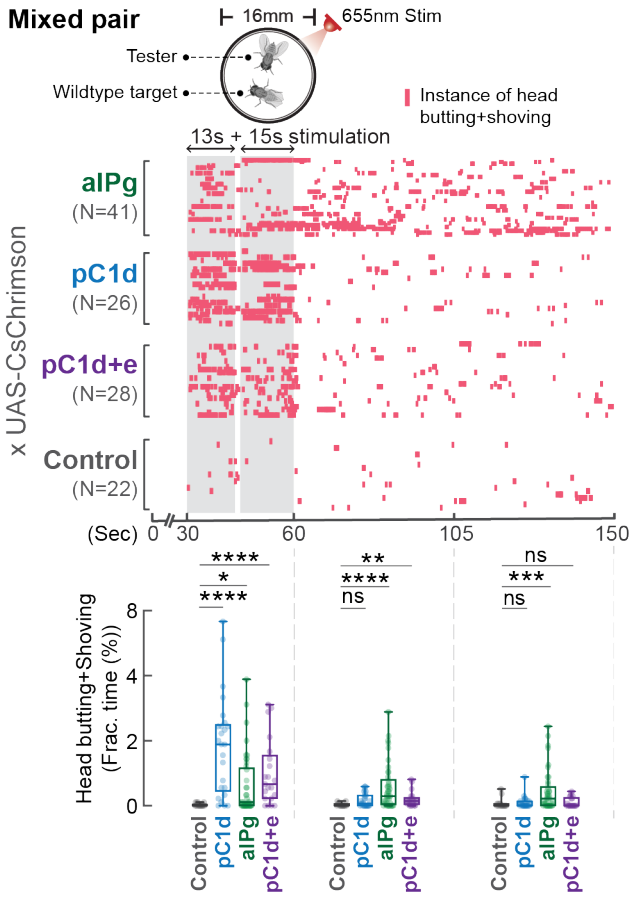

Fig. S3. Stimulation of aIPg, but not pC1d alone promotes persistent attacks toward a wild-type target. (A) Testers remained aggressive toward a group housed wild-type target after the cessation of aIPg stimulation, but aggression was time-locked to the stimulation period when pC1d neurons were stimulated. Aggression (head butting+shoving, red ticks) was shown in the raster plot, and the fraction of time spent on attacks was compared in the box plot. Flies were freely interacting throughout the experiments, and data were combined from two independent biological repeats. ****p<0.0001; ***p<0.001; **p<0.01; *p<0.05; ns, not significant. Control, empty split-Gal4 driver (BDP-AD; BDP-DBD).

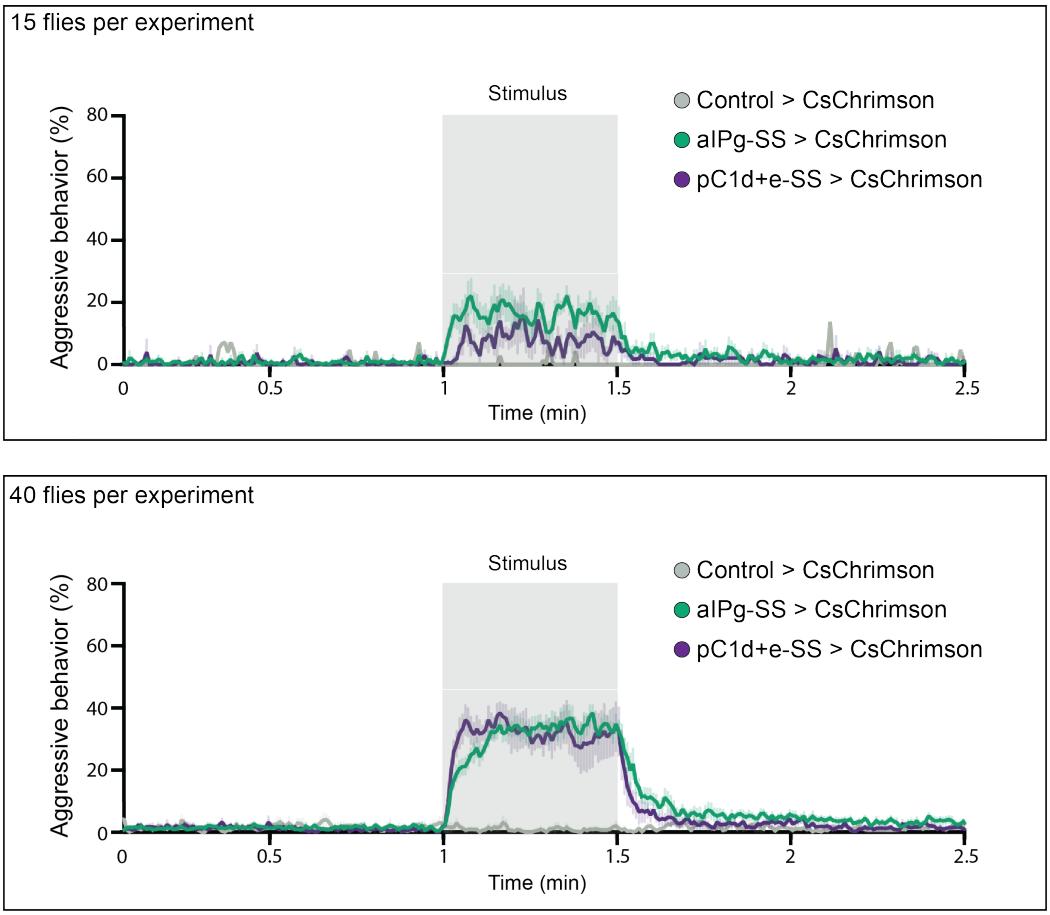

Fig. S4. Density influences the persistence of aggression. Aggression increased and persisted longer after stimulation with increased fly density in the behavioral chambers. For each experiment, 15 (top) or 40 (bottom) flies were placed in the behavioral chamber. Percentage of flies performing aggressive behavior at a given frame is shown by the color-coded traces. Data were combined from two independent biological repeats. Green, aIPg-activated flies. Purple, pC1d-activated flies. Grey, Control flies (empty split-Gal4 driver, BDP-AD; BDP-DBD). (A) Control > CsChrimson, n = 1 experiment; aIPg-SS > CsChrimson, n = 7 experiments; pC1d+e-SS > CsChrimson, n = 4 experiments; (B) Control > CsChrimson, n = 4 experiments; aIPg-SS > CsChrimson, n = 11 experiments; pC1d+e-SS > CsChrimson, n = 7 experiments.

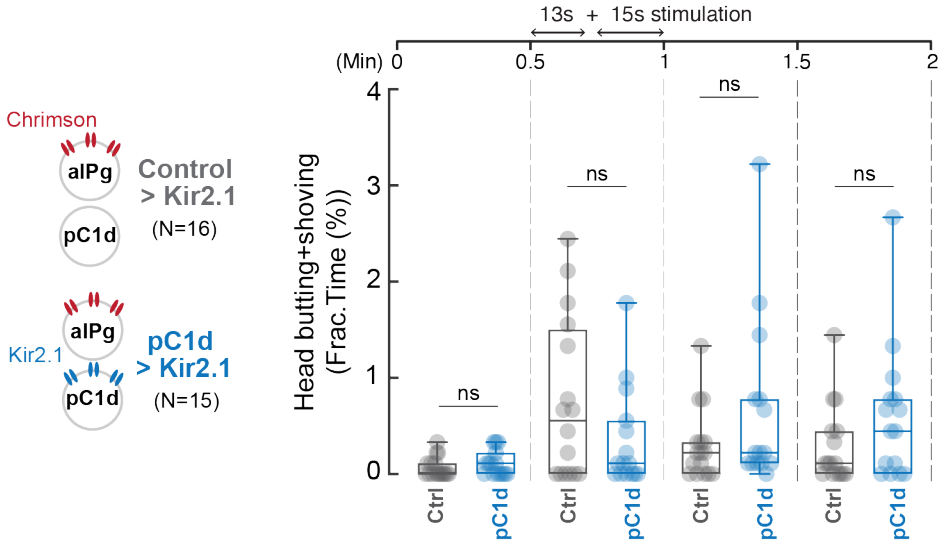

Fig. S5. Inhibition of pC1d activity does not alter aIPg-induced aggressive behavior. Blocking pC1d activity by Kir2.1 expression did not significantly change persistent behavior induced by aIPg activation. Fraction of time spent performing aggressive behaviors as shown in raster plots in Figure 3. Flies were freely interacting throughout the experiments, and the data were combined from two independent biological repeats. The differences between Control > Kir2.1 and pC1d > Kir2.1 groups in the separate 13s and 15s stimulation periods were not significant (13s period, p = 0.2978; 15s period, p = 0.6650). ns, not significant. Control, empty split-Gal4 driver (BDP-AD; BDP-DBD).

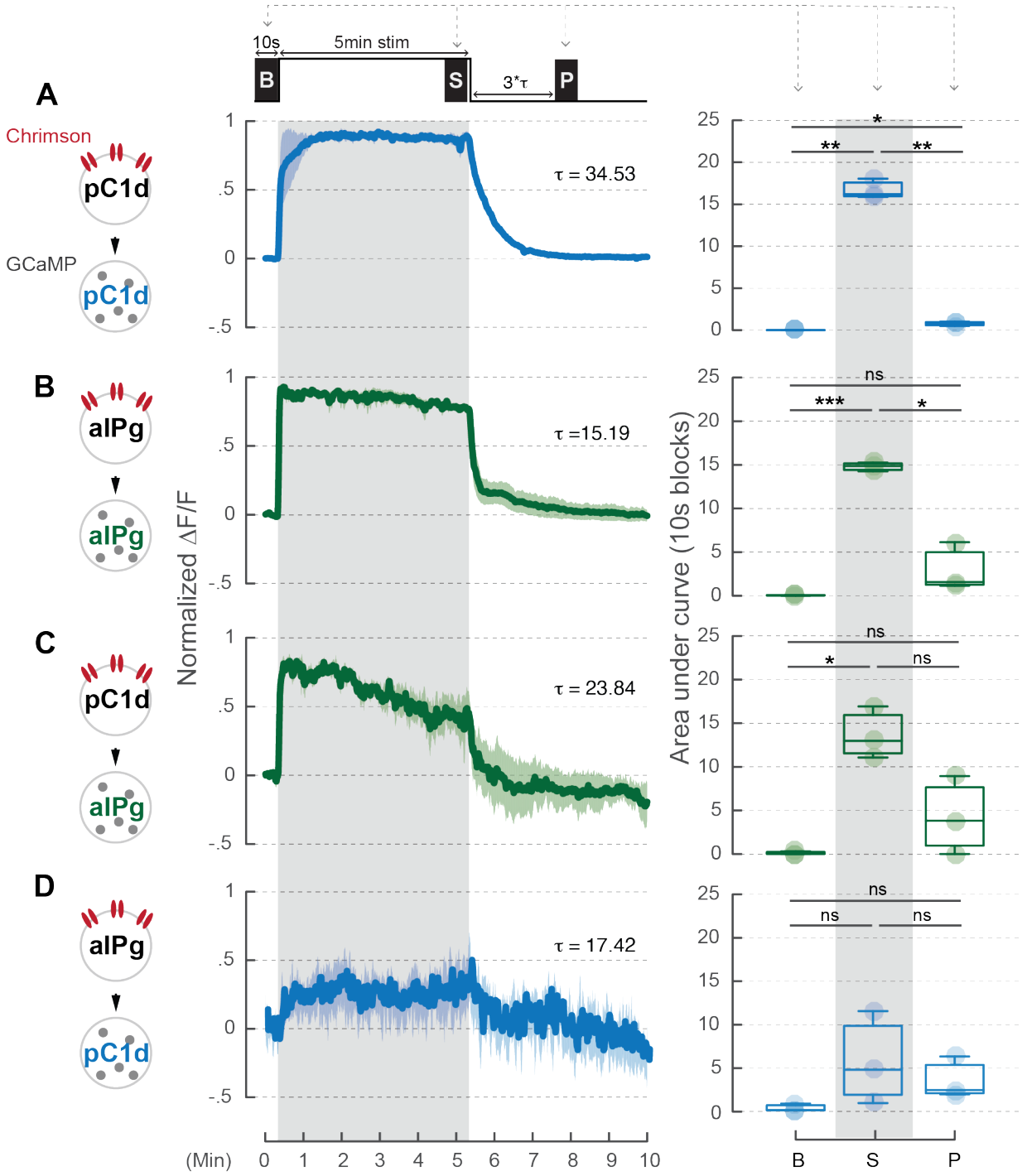

Fig. S6. A 5-minute stimulation of pC1d neurons does not induce prolonged activity in alPg neurons. pC1d (A or C) or alPg (B or D) neurons were activated for 5 minutes. The blue and green traces showed the GCaMP signals in either pC1d or alPg neurons, respectively. Dark blue/green line, mean. Light blue/green line, SEM. Area under the GCaMP trace during the 10 second blocks in the baseline (B), stimulation (S), and post-stimulation (P; 3 times Tau after stimulation) period were compared in the box plots. Data were combined from three to four independent biological repeats. Light blue/green circle, individual data. ***p<0.001; **p<0.01; *p<0.05; ns, not significant.